ACS Synthetic Biology
Research Article
Cite This: ACS Synth. Biol. 2019, 8, 1776−1787
pubs.acs.org/synthbio

Bacterial MbtH-like Proteins Stimulate Nonribosomal Peptide Synthetase-Derived Secondary Metabolism in Filamentous Fungi

Reto D. Zwahlen,[†] Carsten Pohl,[†,∥] Roel A. L. Bovenberg,[‡,§] and Arnold J. M. Driessen*[,†]

[†]Molecular Microbiology, Groningen Biomolecular Sciences and Biotechnology Institute, University of Groningen, 9747 AG Groningen, The Netherlands

[‡]Synthetic Biology and Cell Engineering, Groningen Biomolecular Sciences and Biotechnology Institute, University of Groningen, 9747 AG Groningen, The Netherlands

[§]DSM Biotechnology Centre, 2613 AX Delft, The Netherlands

Supporting Information

ABSTRACT: Filamentous fungi are known producers of bioactive natural products, low molecular weight molecules that arise from secondary metabolism. MbtH-like proteins (MLPs) are small (∼10 kDa) proteins, which associate noncovalently with adenylation domains of some bacterial nonribosomal peptide synthetases (NRPS). MLPs promote the folding, stability, and activity of NRPS enzymes. MLPs are highly conserved among a wide range of bacteria; however, they are absent from all fungal species sequenced to date. We analyzed the interaction potential of bacterial MLPs with eukaryotic NRPS enzymes first using crystal structures, with results suggesting a conservation of the interaction surface. Subsequently, we transformed five MLPs into *Penicillium chrysogenum* strains and analyzed changes in NRPS-derived metabolite profiles. Three of the five transformed MLPs increased the rate of nonribosomal peptide formation and elevated the concentrations of intermediate and final products of the penicillin, roquefortine, chrysogine, and fungisporin biosynthetic pathways. Our results suggest that even though MLPs are not found in the fungal domain of life, they can be used in fungal hosts as a tool for natural product discovery and biotechnological production.

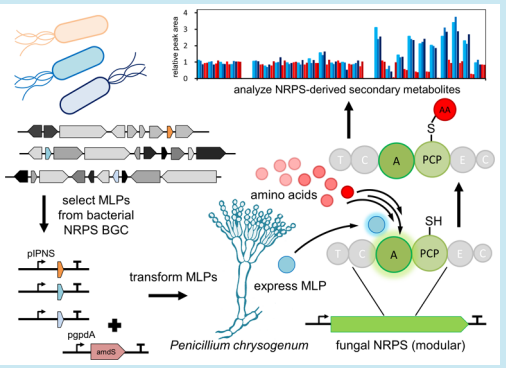

KEYWORDS: *MbtH-like protein, nonribosomal peptide synthetases, Penicillium chrysogenum, secondary metabolism, fungal natural products*

Nonribosomal peptides (NRP) are a class of peptide secondary metabolites produced by filamentous fungi and a subset of bacteria.[1] NRPs are synthesized by nonribosomal peptide synthetases (NRPS), which are highly structured and complex enzymes, closely related to other modular enzymes such as polyketide synthetases (PKS), NRPS-PKS hybrid synthetases, and fatty acid synthetases (FAS). They have certain distinct properties in common, the most striking one being their structural organization in modules and domains, which reflects their shared evolutionary history.[2] Typically, each module consists of an adenylation (A), thiolation (T), and condensation (C) domain to select, activate, transfer, and condensate a specific substrate amino acid, respectively. In addition, modules can contain optional domains for substrate methylation, epimerization, macrocyclization, and thioesterification, with the latter being relevant for final nonribosomal peptide (NRP) product release.[3] Consequently, the structural diversity of NRPs is tremendous. It has been estimated that about 500 naturally occurring amino acids and carboxylic acids may serve as substrates for NRPS enzymes to form small bioactive peptide scaffolds.[4,5] The natural functions of NRPs are as diverse as their structures. They are involved in signaling, communication, metal ion chelation, and host protection. NRPs have important pharmaceutical functions as antibiotics, antifungal agents, immunosuppressants, as well as cytostatic drugs.[6−8]

To facilitate the complex biochemistry of NRP formation in a cellular environment, two types of activating and chaperoning factors for NRPS have been reported in literature to date. *Sfp*-type phosphopantetheinyl transferases (Pptases)[9] activate both bacterial and fungal NRPS enzymes by phosphopantotheinylation of the T domain active site.[10,11] Typically, different classes of Pptases exist with narrow and broad substrate specificities and their corresponding genes are conserved in one or multiple genomic copies across organisms.[3] They are normally not part of a secondary metabolite biosynthetic gene cluster (BGC). MbtH-like proteins (MLPs) are relatively small (below 10 kDa) and associate with the adenylation domain of NRPS enzymes.[12−15] Initially discovered in *E. coli* as part of the enterobactin BGC,[16] MLPs were named after the

Received: March 13, 2019
Published: July 8, 2019

DOI: 10.1021/acssynbio.9b00106
ACS Synth. Biol. 2019, 8, 1776−1787

Table 1. Overview of MLP Variants Tested in This Study[a]

name	UniProt	organism	biosynthetic gene cluster	GenBank ID	reference
ComB	Q93N85	*Streptomyces lavendulae*	Complestatine	AF386507	61
CdaI	Q7BRC2	*Streptomyces coelicolor*	Calcium dependent antibiotic	AL939115	62
Tcp13	Q70AZ5	*Actinoplanes teichomyceticus*	Teicoplanin	AJ605139	63
Veg8	B7T1C1	uncultured soil bacterium	putative (vancomycin-like eDNA derived gene cluster, VEG cluster)	EU874252	64
Teg7	B7T1D2	uncultured soil bacterium	putative (teicoplanin-like eDNA derived gene cluster, Teg cluster)	EU874253	64

[a]MLPs were selected and characterized for their interaction potential with fungal NRPS from *Penicillium chrysogenum*.

gene MbtH in the BGC encoding the iron-chelating siderophore mycobactin (Mbt) in *Mycobacterium tuberculosis*.[17] It has become increasingly apparent that MLPs play a key role in bacterial NRPS function.[13−15,18] In bacteria, MLP genes can cluster with genes of an NRP-coding BGC suggesting coexpression and specificity; however, certain MLPs seem to be less specific and can interact with multiple NRPS,[19−21] presumably due to a generic, but not yet resolved chaperoning effect. Upon binding, MLPs not only enable or enhance the NRPS adenylation activity,[13] but also increase the solubility of NRPS enzymes,[14,15,22] which are often the largest proteins in bacteria. Despite the essential function MLPs fulfill for some bacterial NRPSs,[17,23] they appear completely absent from any fungal genome sequenced up to date. Therefore, the introduction of MLPs in a fungal host might increase the functional expression and activity of fungal NRPS and possibly fungal NRP formation.

Here, we have analyzed and tested five bacterial MLPs from various bacterial sources to evaluate their impact on the activity of NRPS enzymes in the filamentous fungus *Penicillium chrysogenum*. This fungus is most prominently known as industrial producer of β-lactam antibiotics,[24,25] but in addition produces various other secondary metabolites. Remarkably, three tested bacterial MLPs stimulated the formation of nonribosomal peptides, showing improved kinetics and elevated levels of secondary metabolites, including the primary NRP products. This study shows for the first time that bacterial MLPs can be utilized to enhance secondary metabolism in eukaryotes, specifically a fungal host, providing a potentially new approach for increasing the yield of fungal NRPs.

RESULTS AND DISCUSSION

Modeling of Conserved Residues for Interaction of Bacterial MLPs and Fungal NRPS. In order to explore the potential of bacterial MLPs to interact with eukaryotic NRPSs, possible cocomplexes were modeled. MLPs display a high degree of structural conservation,[4] and several structures are available displaying an A-domain−MLP interface: the NRPS SlgN1,[26] involved in biosynthesis of Streptolydigin in *Streptomyces lydicus* (ATCC 25470), EntF[27,28] which produces enterobactin in *E. coli* (*i.e.*, strain JM109), the NRPS TioS from *Micromonospora sp. ML1* in complex with its MLP TioT that is part of the thiocoraline BGC,[29] and the dimodular NRPS DhbF in contact with the clustered MLP ADP73024.1[30] from *Geobacillus sp. Y4.1MC1*, producing bacillibactin. All structures highlight the same potential interaction region, but the structure of SlgN1 lacks an A_{sub} domain and, in contrast to EntF, possesses a covalently linked MLP. These observations suggest the existence of a defined and conserved part of the A_{core} surface which enables the dynamic association of different MLP variants. Therefore, only the SlgN1 structure in complex with an MLP was used as a template in the modeling.

Furthermore, 5 MLPs were selected. Teg7 and Veg8 stem from a metagenomic screen of soil bacteria, Tcp13 from *Actinoplanes teichomyceticus* and CdaI and ComB are from *Streptomycetes sp.* (Table 1). Adenylation domains were extracted from 3 NRPS enzymes present in the filamentous fungus *Penicillium chrysogenum*. These are the L-δ-(α-aminoadipyl)-L-cysteinyl-D-valine synthetase ACVS[31−33] (3 A-domains) which synthesizes L-δ-(α-aminoadipyl)-L-cysteinyl-D-valine (LLD-ACV), the tripeptide precursor of penicillin; RoqA (2 A-domains), the NRPS synthesizing histidyltryptophanyldiketopiperazine (HTD), which is further converted into a series of roquefortine and meleagrin derivatives[34−37] and ChyA (2 A-domains), which is responsible for the formation of 2-(2-aminopropanamido)benzoic acid,[38] which is further converted into chrysogine.[39,40]

RaptorX and SWISS-MODEL served as a basis for the creation of *in silico* structural models of MLPs and A-domains and validated against 23 PDB templates of 16 proteins (Supporting Information 1). Global Model Quality Estimates (GMQE, between 0−1) were calculated, resulting in a median GMQE of 0.62 ± 0.076 for A-domains and 0.76 ± 0.47 for MLPs (Supporting Information 2). The obtained models were structurally aligned to SlgN1 (PDB: 4GR4) using PyMOL, both in a global and interface directed fashion. Due to the absence of an A_{sub} domain in 4GR4, only the 340 A_{core} residues of SlgN1 were used for alignment, covering the hypothetical A-domain−MLP interface. The process allowed for an alignment of up to 305 (of 340) Cα carbons in fungal-NRPS−SlgN1 models and 59 (of 61) in MLP−SlgN1 models, with low Root Mean Square Deviation errors (RMSD, Supporting Information 3), indicating a structural similarity. Next, A-domains and MLP sequences were aligned to the corresponding templates and the secondary structure was extracted from the model and compared (see Figure 1a,b). Additionally, potential interface forming (IF) and interactive (IA) residues were determined, according to the SlgN1 structure. This accounted to 29 IF and 6 IA residues on the MLP domain and 32 IF and 12 IA residues on the adenylation domain, respectively.

The alignment revealed that the selected MLPs displayed a high count of 20 to 23 conserved IF residues (of 29) and are conserved for all 6 IA residues (Figure 1c). With respect to the fungal A-domains, 8−13 (of 32) IF and 4−10 (of 12) IA residues are conserved (Figure 1d). The region resolving around α-helix 11 and β-sheet 22 (in SlgN1 4GR4) on the A-domain furthermore includes two core alanine residues at position 428 (A428) and 433 (A433), centered at the interface area. Although A433 seems to be completely absent from all investigated fungal A-domains, ACVS M2 and RoqA M2 both contain an alanine at position 428. Especially the A-domain of ACVS M2 appears to have a high similarity to SlgN1. With respect to the MLPs, not only the A428/A433 interacting partners Ser23 and Lys24 are conserved, but all MLPs contain the minimal MLP functionality motif (Figure 1d). Overall, the

DOI: 10.1021/acssynbio.9b00106
ACS Synth. Biol. 2019, 8, 1776−1787

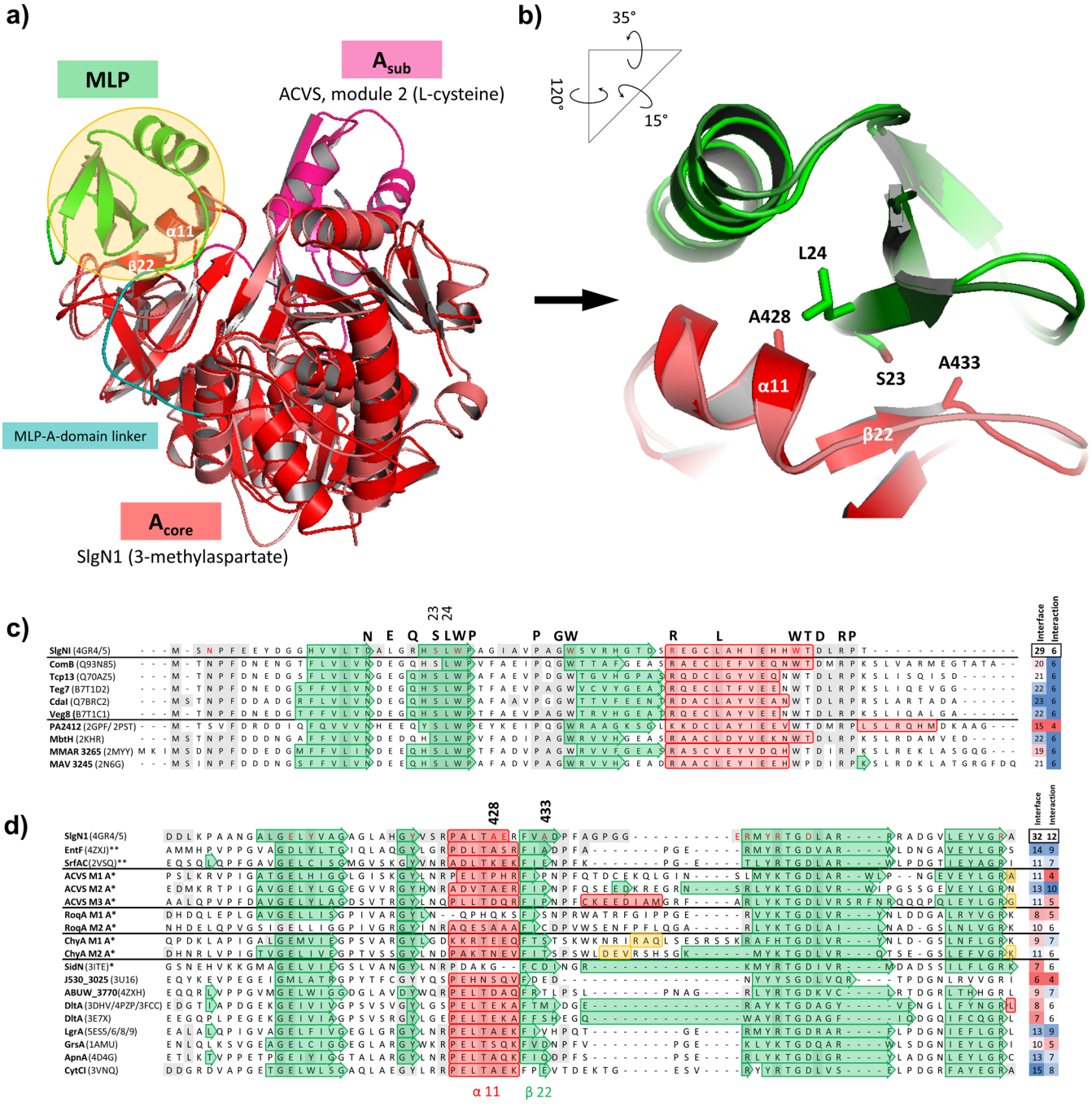

Figure 1. Structural model comparison and alignment of SlgN1 with ACVS and ComB MLP. (a) Structural alignment of SlgN1 (PDB: 4GR4; A_{core}-domain: red; MLP-A-domain-linker: blue) with refined A_{sub} model (pink) of an ACVS M2 model (GMQE = 0.80) and ComB MLP (green). The structural alignment of SlgN1−ACVS M2 A indicates a structurally conserved interface, shown in more detail in (b). (b) Structural alignment as in (a) with a focus on the core binding structure α-11 and β-22 as well as conserved residues S23, L24 and possible interactive residues A428 and A433 (indicated in the A-domain and MLP alignments in (c) and (d)). The alignments cover all relevant residues for interface formation and interaction as compared to SlgN1 (PDB: 4GR4). (c) Alignment of five MLPs used in this study and templates for model generation in SWISS-model. Conservation of IA and IF residues is indicated in the utmost right column. The essential[65] MLP motif is shown in bold above the aligned sequences. (d) Alignment of 7 fungal A-domains (*) alongside all relevant templates used for the generation of the models, including common gene names and PDB entry. Sequences with MLP dependency according to STRING[66] are indicated (**). Extracted secondary structures of all proteins are colored, showing α-helixes (red), β-sheets (green) and 3_{10}-helixes (yellow).

MLPs structures are highly conserved and are composed of 3 antiparallel β-sheets and one α-helix. The most significant differences were found in the disordered N-terminus, which is not involved in A-domain-MLP interactions. A more diverse secondary structure topology was observed between fungal A-domains. Although the upstream region of α-helix 11 appears reasonably conserved, an additional short insertion (10 to 15 residues) is found upstream of β-sheet 22 in all *P. chrysogenum* A-domains tested here. However, this does not seem to interfere with any hypothetical interacting residues as further underlined by the high degree of structural agreement of the ACVS M2 A-domain and ComB MLP with SlgN1 when

DOI: 10.1021/acssynbio.9b00106
ACS Synth. Biol. 2019, 8, 1776−1787

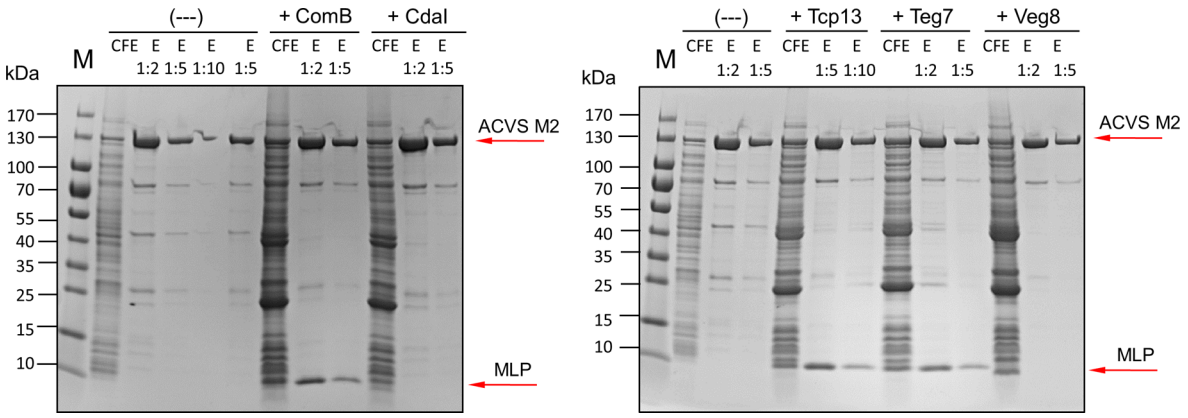

Figure 2. MLPs copurify with ACVS M2. ACVS module 2 (M2) from *N. lactamdurans* and MLPs were coexpressed, and ACVS M2 was purified using the C-terminal His_6-Tag. The NRPS module and the MLPs are indicated with red arrows. The copurification pattern separated by denaturing SDS-PAGE shows that ComB, Tcp13, and Teg7 can interact and show strong interactions with the A-domain. M = marker; CFE = cell free extract; E = elution fraction, 1:2 or 1:5 diluted.

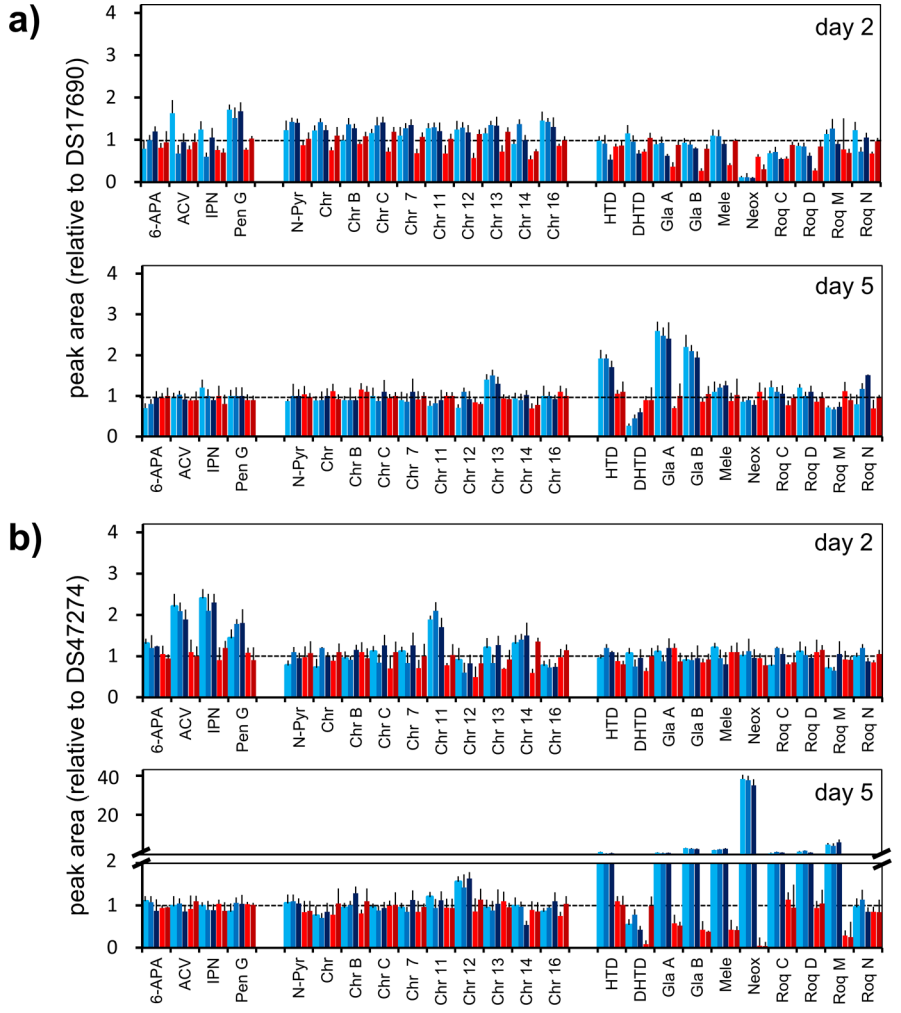

Figure 3. Secondary metabolite formation by MLP strains. Different MLPs genes were randomly integrated into the genome two *P. chrysogenum* strain lineages, and changes of NRPS-derived extracellular metabolites were quantified relative to the parental strain. Peaks were identified according to accurate mass and retention time and normalized for dry weight of the cultures. Strains are separated by their parental origin (a) DS17690 and (b) DS47274 and day of fermentation. Each bar represents the mean change of the peak area of a given metabolite relative to the parental strain and was calculated from at least 3 independent biological replicates, represented as (DS17690/DS47274): ComB (light blue; 10/12), 12 Tcp13 (medium blue; 7/5), 10 Teg (dark blue; 6/4), CdaI (brown; 4/6) and Veg8 (red; 5/3). Abbreviations of metabolites and acquired *m/z* values are included in Supporting Information 8.

DOI: 10.1021/acssynbio.9b00106
ACS Synth. Biol. 2019, 8, 1776−1787

superimposed (Figure 1a). In spite of the absent A_{sub} domain in SlgN1, the remaining analogous structures align well and the local interface alignment reveals a good positioning of α-helix 11 and β-sheet 22 (Figure 1b) at the core interface. In conjunction with the MLP conservation and the very concise NRPS A-domain−SlgN1−MLP superposition, this data indicated that also fungal NRPS are potentially capable of interacting with bacterial MLPs

Copurification of Bacterial MLPs with NRPS Enzymes *in Vitro*. To validate the *in silico* predicted A-domain-MLP interaction, *in vitro* copurification experiments were attempted by coexpressing the cysteine-linking module (M2) of the *P. chrysogenum* NRPS ACVS in combination with one of 5 different MLPs in *E. coli*. Because of the poor expression of *P. chrysogenum* ACVS M2, modules of the functionally conserved bacterial ACVS from *Amycolatopsis lactamadurans* were subsequently cloned and tested because of the high degree of A-domain homology with the fungal enzyme and no reported interactions with MLPs. *A. lactamadurans* ACVS M2 could be expressed successfully in *E. coli* along with one of the MLPs and was purified *via* a C-terminal added His-tag and visualized using SDS-PAGE. Despite the considerable high level of MLP conservation, a distinct copurification pattern emerged (Figure 2 and Supporting Information 4): ComB, Teg7, and Tcp13 all copurified significantly with ACVS module 2 while CdaI and Veg8 failed to copurify both with the ACVS module and the full-length protein. This could imply that none of the 3 A-domains presented to CdaI and Veg8 was accepted as an interaction partner, possibly because of a more stringent specificity of CdaI and Veg8. Strikingly, all five MLPs tested here do not show a high divergence in their amino acid sequences nor any specific differences except the variable C-terminus to explain the mechanisms shaping two classes of interacting and noninteracting MLPs as observed here. A variation of performance across similar MLPs was also observed by Schomer and co-workers[41] when testing MLP interactions with the enterobactin NRPS EntF. It is important to note that the coexpression of MLPs did not result in an improvement of soluble M2 and full length ACVS protein levels (Figure 2 and Supporting Information 4). This is in part expected since no ACVS containing BGC were identified that contain an MLP. These data demonstrate that the ACVS is indeed capable of interacting with MLP proteins, validating the structural analysis.

Bacterial MLPs Increase Titers of Fungal NRPS-Derived Products in *P. chrysogenum*. To examine the impact of the bacterial MLPs on secondary metabolite formation in a fungal host, 5 MLP candidates were transformed into *P. chrysogenum* using appropriate expression cassettes and a nontargeted genome insertion strategy. *P. chrysogenum* strain DS17690 emerged from a classical strain improvement program (CSI) aimed to optimize penicillin production and contains 8 copies of the penicillin BGC, while strain DS47274 is derived from DS17690 but only contains a single penicillin BGC.

The presence of MLP variants in strains was verified using colony PCR (Supporting Information 5). Strains were grown in submerged culture using medium supplemented with phenylacetic acid for production of penicillin G. Culture supernatant at day 2 and 5 was subjected to secondary metabolites profiling using LC−MS. Subsequently, peak areas of final and intermediate metabolites of the NRPS BGCs responsible for biosynthesis of penicillin (ACVS − Pc21g21390), chrysogine (ChyA − Pc21g12630) and roquefortine (RoqA − Pc21g15480) were quantified and normalized by dry weight. LC−MS analysis of total ion chromatograms revealed major changes in the extracellular metabolic profile of both *P. chrysogenum* DS17690 and DS47274 borne MLP containing strains (Supporting Information 6). This concerned primarily products of the chrysogine, penicillin and roquefortine BGCs but also other, less well characterized compounds. Upon inspection of all combinations of strains, peak areas of several compounds associated with the aforementioned pathways significantly increased relative to the parental strains lacking the MLPs (Figure 3). We also obtained strains that showed lower NRPS product levels, but this likely is a side effect of the nontargeted genomic insertion strategy of the MLPs employ to generate the strains.

A notable difference between the two strain backgrounds DS47274 and DS17690 was observed, showing overall stronger effects in the lower penicillin producing DS47274 strains as compared to the high yielding DS17690 strains. DS47274 strains expressing MLPs showed positive effects on the penicillin, roquefortine and chrysogine biosynthesis, while DS17690 borne strains experience the strongest effects on penicillin derived metabolites. The stimulatory effect on NRPS products was also observed for the initial, NRPS-derived metabolites LLD-ACV and HTD, which are significantly increased in most of the DS47274 strains and to a lesser degree in DS17690 strains. Increased levels of roquefortine-related compounds were maintained on day 5 of cultivation, while the chrysogine-related compounds, which were detectable after 2 days of fermentation were less abundant on day 5 (Figure 3). Overall, strains containing Tcp13, Teg and Com produced an increased level of NRPS-derived metabolites while CdaI and Veg8 bearing strains did not show a significant change in NRPS products.

ComB MLP Performance for Production of LLD-ACV and HTD in *P. chrysogenum*. Strains derived from DS17690 (3) and DS47274 (5) carrying the ComB MLP were further characterized for *pcbAB* and *com* gene copy numbers as well as *com* expression at 2 and 5 days of the fermentation (Figure 4). All strains contained one copy of the *com* gene, except for DS47274 7.1 and 8.1, which contain 5 and 8 copies of *com*, respectively (Figure 4b). Furthermore, DS47274 strains contain one copy of *pcbAB*, while DS17690 strains contain 6−8 copies (Figure 4a). The *com* expression profile of the selected strains 1.2; 2.4 (8x*pcbAB*) and 7.3; 8.1 (1x*pcbAB*), indicates that the gene is well expressed after 2 and 5 days and that the expression increases with the copy number (Figure 4c). The strains were subjected to shake flask cultivation and metabolite profiling (Figure 5). Again, various secondary metabolites were affected, in particular the penicillin and chrysogine related metabolites in both DS17690 and DS47274 increased after 2 days, with the most pronounced effect in DS47274. For roquefortine metabolites, levels increased most pronounced in DS47274 strains after 5 days. The ComB-dependent effect on penicillin production levels causes an earlier onset of production, *i.e.*, after 2 days of fermentation, whereupon it stabilizes to the levels found in the parental strain after 5 days. A similar behavior is observed with the chrysogine related metabolites, whereas the production of roquefortine-related compounds is stimulated in the later stages of fermentation, *i.e.*, after 5 days (Figure 5). The levels of ACV were additionally quantified and corrected for cell dry weight (CDW) (Figure 6a). The RoqA derived product HTD increased up to 3.1- and 1.9-fold in strain DS47274 and DS17690, respectively (Figure 6b). Extracellular levels increased from 0.14 μmol/g(CDW) in DS47274 up to 0.70

DOI: 10.1021/acssynbio.9b00106
ACS Synth. Biol. 2019, 8, 1776−1787

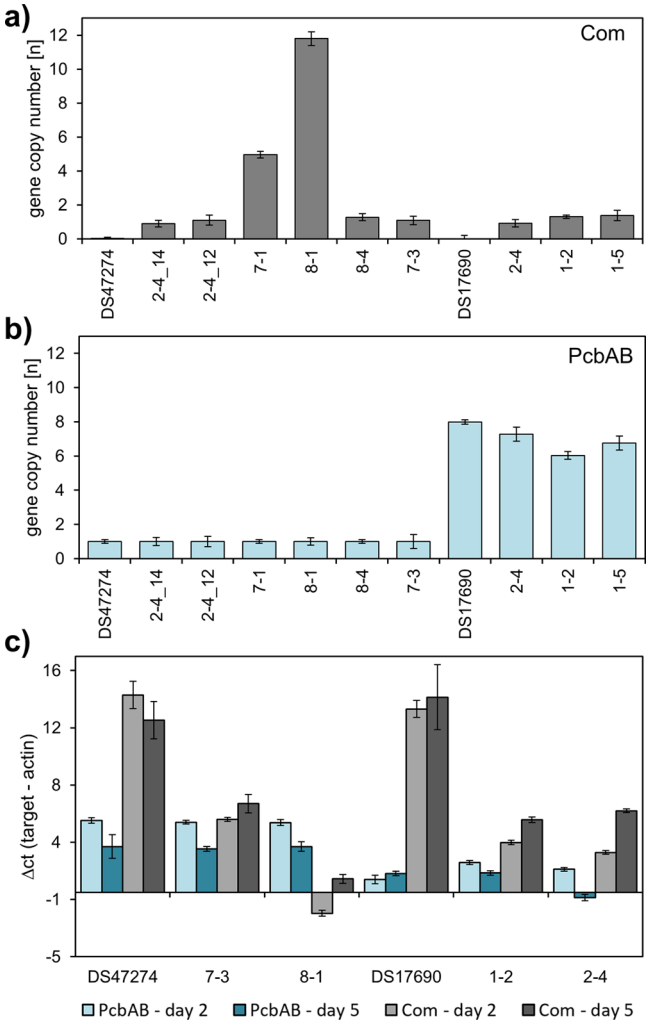

Figure 4. Characterization of gene expression and gene copy numbers in strains with the ComB MLP. Determination of *com* (a) and *pcbAB* (b) gene copy number and expression in selected strains (c). Strains are displayed in a separated manner, showing DS17690 (8 copies of *pcbAB*, right) and DS47274 (1 copy *pcbAB*, left) strain backgrounds apart. Expression of *com* and *pcbAB* on day 2 and 5 of cultivation in shake flasks is displayed as d(ct) of the target gene *versus* actin to be able to compare wild-type samples without COM. Relative changes in gene expression for *pcbAB* and other relevant NRPS (*chyA* and *roqA*) genes are included in Supporting Information 7. Error bars represent standard deviation of two biological replicates and two technical replicates each.

in the DS47274 ComB MLP strain 2−4_12 at day 2 and 0.61 to 1.48, in DS17690 and DS17690 ComB MLP strain 2−4, respectively. All these observed effects are not related to changes in expression of the NRPS enzymes as indicated by the qPCR data. (Supporting Information 7).

Strain Lineage and Secondary Metabolite Fingerprint Impact Effect of ComB MLP. A more controlled approach for integration was performed in two other strain backgrounds, the penicillin-cluster free strain DS68530 and DS68530res13, a strain where production of the polyketide sorbicillin and related compounds was restored by reverting a point mutation in the PKS gene *pks13* (Pc21g05080).[42,43] The analysis now also included the fungisporin products of the 4-modular non-canonical NRPS HcpA[44] (Pc1604690). Fungisporin and related cyclic tetrapeptides are only produced in trace amounts when the penicillin BCG is present. In penicillin-cluster-free strains, product formation is observed late in fermentation (after 5 days) due to low *hcpA* expression.[44]

In both strains, targeted, nuclease-stimulated[45] integration of the ComB MLP construct into the intergenic region[46] between Pc20g07090 and Pc20g07100 was performed. Strains were purified and grown in penicillin production media without phenylacetic acid and the levels of chrysogine, roquefortine, fungisporine and sorbicillin related products were quantified after 5 days and compared to the parental strains (Figure 7). Again, an increase in metabolite levels across all NRPS product classes was observed in DS68530 (Figure 7a), but the pattern differed when compared to the penicillin producing DS17690 and DS47274 strains. This can be explained by changes in primary metabolite availability and altered NRPS gene expression when strains are grown in the absence of phenylacetic acid.[24,47] Remarkably, in the strain containing the restored sorbicillin BCG, *i.e.*, DS68530res13, ComB MLP had little effect on the production of NRPS-derived metabolites (Figure 7b). This strain, however, in general shows only low levels of NRPs, likely because the sorbicillin BGC competes for cellular resources for NRP production. Taken together, these observations demonstrate that bacterial MLPs stimulate NRP production in filamentous fungi.

CONCLUSIONS

This study demonstrates for the first time that expression of bacterial MLPs can improve the biosynthesis of NRP-derived secondary metabolites in filamentous fungi, as demonstrated for *Penicillium chrysogenum*. Modeling of the MLP interaction with the A-domains of three fungal NRPS suggests that many of the directly interacting residues are conserved in the analyzed fungal A-domains. Indeed, elevated levels and improved kinetics of NRP formation were observed when three different MLPs were expressed in *P. chrysogenum*. Moreover, the presence of ComB MLP increased the metabolite levels of four individual NRP pathways, suggesting the existence of a transferable effect and potentially low A-domain interaction stringency for ComB. However, it was also observed that CdaI and Veg8 did not show any copurification with the ACVS NRPS, pointing to a very stringent preference for A-domains. Since the analysis of interacting amino acids in both MLP and NRPS A-domains did not reveal any obvious bias between functional and none-functional MLPs, further studies are needed to identify the underlying mechanism separating these two groups. An interesting MLP to test in future studies for their applicability in fungal hosts would be the MLP MXAN_3118 found in *Myxococcus xanthus* DK1622.[48] MXAN_3118 is not associated with a NRPS BGC but was found to interact with seven different NRPS enzymes, making MXAN_3118 a promising "universal" MLP. Despite different MLPs have to be tried for a specific product, given their small size, all MLPs can be incorporated with little effort and expression burden into an eukaryotic screening or production host. Thus, MLPs provide an interesting new tool for both native and heterologous BGC expression in fungal strains or can be applied in biotechnological manufacturing processes of NRP-derived metabolites. Furthermore, this MLP-dependent effect could be of value for the discovery of NRPS derived cryptic or low-abundance NRP metabolites with potentially relevant bioactivities.

DOI: 10.1021/acssynbio.9b00106
ACS Synth. Biol. 2019, 8, 1776−1787

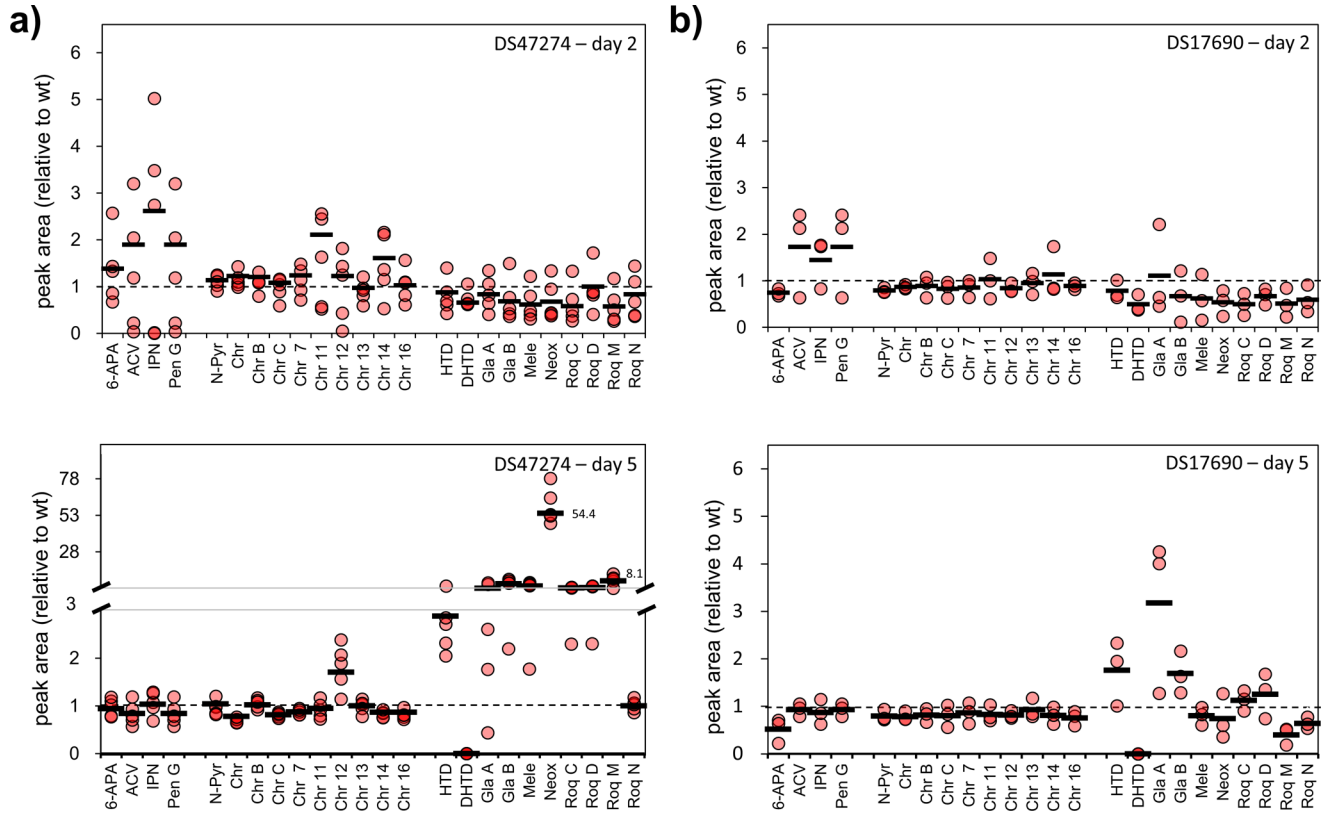

Figure 5. Changes of NRPS-derived extracellular metabolites in the ComB MLP expressing strains. Changes in extracellular metabolites in strains expressing ComB MLP compared to the parental strain DS47274 (a) or DS17690, respectively (b) after 2 and 5 days of cultivation using penicillin production medium supplemented with phenylacetic acid (PAA) SMP medium. Each data point represents a single strain. The black bar represents the mean of all strains.

METHODS

Modeling and Molecular Docking. To establish a basis for interaction probabilities of bacterial MLP and eukaryotic NRPS, we utilized *P. chrysogenum* ACV synthetase (PcbAB) as a model NRPS and focused on interactions concerning the adenylation domain (M2 A) of the second module. Adenylation domain boundaries were determined using a prediction by the Conserved Domain Database (CDD) of the NCBI.[49] The obtained sequences were subsequently used to generate models using RaptorX[50] and SWISS-MODEL.[51] Models were classified according to the Model quality (Global Model Quality Estimation, GMQE) and were structurally aligned to SlgN1 (PDB: 4GR5)[26] in a global and interface targeted fashion, respectively, using PyMOL (Schrödinger, 2015).[52] The resulting models were then used for superpositioning and visualization in combination with 4GR4. Finally, a docking analysis was performed using 3DIANA.[53]

Protein Expression Analysis. In order to evaluate interactions, *N. lactamdurans* ACVS was coexpressed with each MLP variant separately. Therefore, the full length *N. lactamdurans* ACVS gene as well as three DNA constructs encoding single ACVS modules were generated, with domain and module borders being determined using the Conserved Domain Database (CCD).[49] Expression of the proteins was performed using the *E. coli* K12 derivative strain HM0079.[54] Cells were grown at 37 °C and 200 rpm to an OD_{600} = 0.6, transferred to 18 °C, 200 rpm for 1 h and subsequently induced using 0.2% L-arabinose (pBAD−ACVS) and 0.3 mM IPTG (pACYCtac−MLP). Cells were collected 18 h after induction by spinning at 3500*g* for 15 min at 4 °C. After resuspension in lysis buffer (50 mM HEPES pH 7.0, 300 mM NaCl, 2 mM DTT, complete EDTA free protease inhibitor; Roche, Basel, Switzerland), cells were disrupted using sonication (6 s/15 s; on/off, 60 cycles, 10 μm amplitude) and cell-free lysate obtained by centrifugation for 15 min 13 000*g* and 4 °C. Enzymes were purified by means of His-tag affinity purification using Ni-NTA beads (Qiagen, Venlo, The Netherlands). Wash steps were performed using two column volumes wash buffer (50 mM HEPES pH 7.0, 300 mM NaCl, 20 mM Imidazole) and a one-step elution using 5 bed volumes elution buffer (50 mM HEPES pH 7.0, 300 mM NaCl, 250 mM Imidazole). Protein concentrations were determined using the BioRad DC assay kit (BioRad, Utrecht, The Netherlands). All fractions were analyzed on 5% SDS-PAGE gels and stained using 0.025% colloidal Coomassie solution. Images were acquired using a FUJIFILM LAS-4000 Scanner (Fujifilm, Tilburg, The Netherlands). Protein levels were additionally compared in-gel by 2-D densitometry using LAS-4000 AIDA software.

Strains. *P. chrysogenum* strains were kindly provided by DSM Sinochem Pharmaceuticals Netherlands B.V. All parental strains[47] used in this study, genotypes, and integration sites of MLPs expression cassettes are listed in Supporting Information 9.

Vector Construction. Cloning was performed using *E. coli* DH5α. Plasmid selection was conducted with 25 μg/mL Zeocin for pIAT and pBAD plasmids and 15 μg/mL chloramphenicol for pACYCtac-MbtH (p15Aori; cat; pTac; lacIq), respectively. All cultures were grown using 2xPY (15 g/L Bacto-tryptone, 10 g/L Yeast extract, 10 g/L Sodium chloride,

DOI: 10.1021/acssynbio.9b00106
ACS Synth. Biol. 2019, 8, 1776−1787

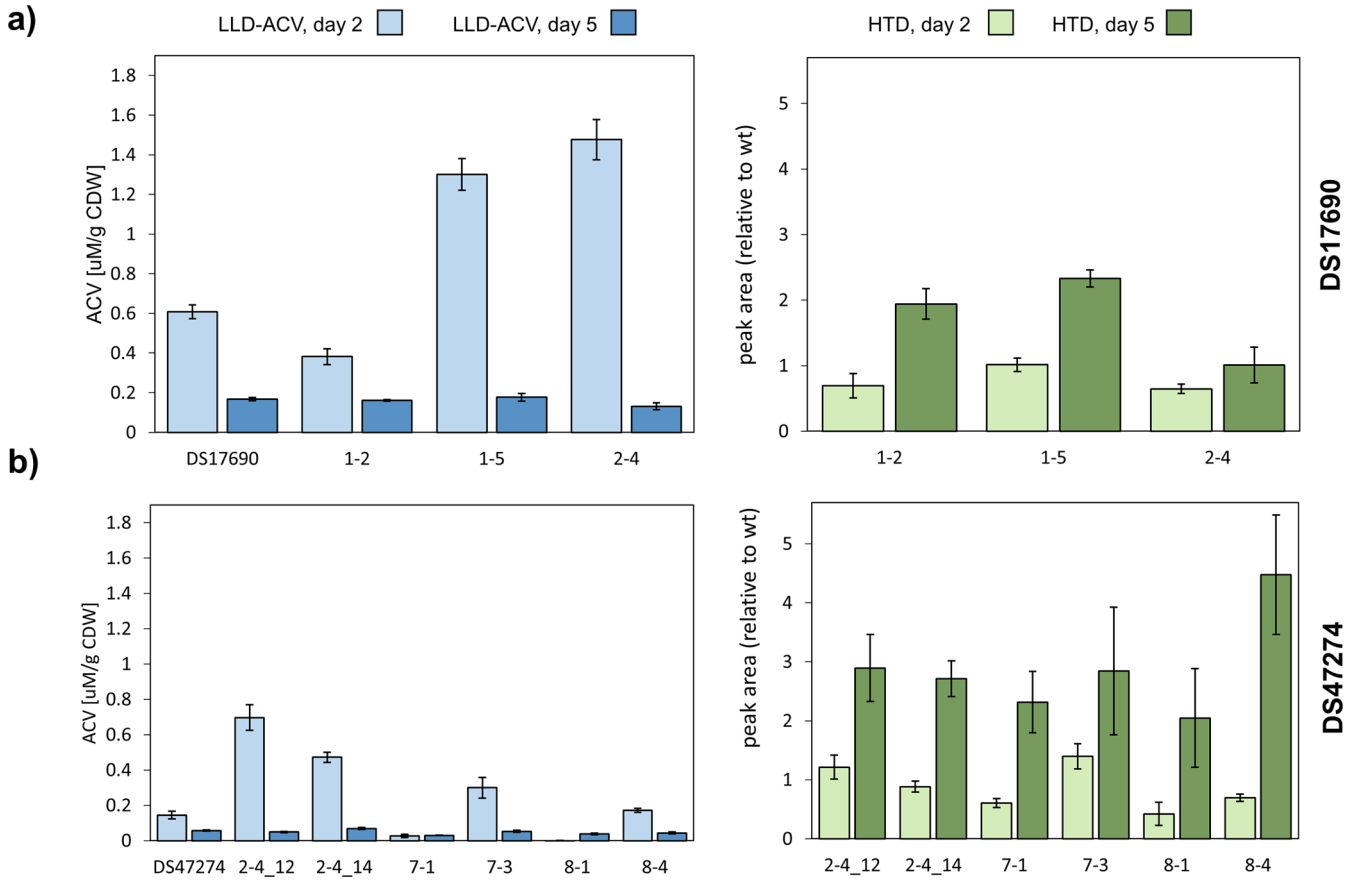

Figure 6. LLD-ACV and HTD changes in ComB MLP expressing strains. Changes of extracellular LLD-ACV (ACVS) and HTD (RoqA) in *P. chrysogenum* strains (a) DS17690 and (b) DS47274. Figures are clustered based on metabolite and strain background and day 2 and day 5; results for each strain are shown in separate bars, derived from two biological and two technical replicates each.

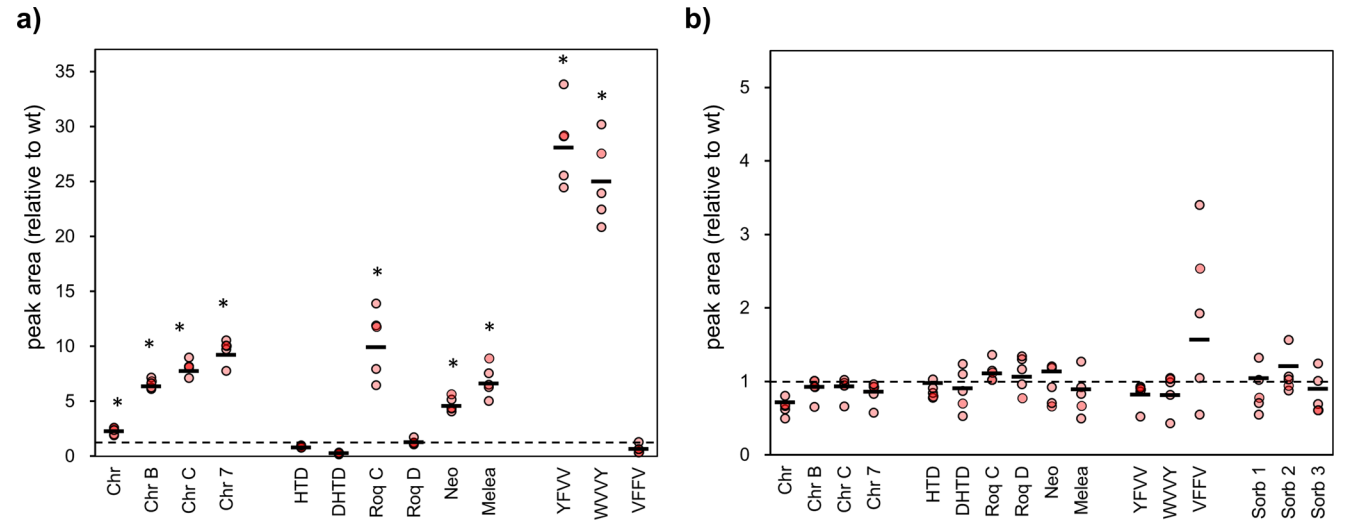

Figure 7. Impact of comB MLP on secondary metabolite level with targeted integration in different strain backgrounds. Levels of chrysogin, roquefortine, fungisporin and sorbicillin-related compounds in fermentation broth were analyzed on day 5 of (a) DS68530 and (b) DS68530res13, capable of producing sorbicillin and related compounds. Sorb1 = sorbicillinol; Sorb2 = dihydrosorbicillinol; Sorb3 = dihydrobisvertinolone. Black bars represent the average of the relative peak area, calculated from 3 individually purified clones (represented as red dots) against the same number of individual parental strain cultures. Asterisks (*) indicates a *p*-value lower than 0.05 (2-sided Student's *t* test). Abbreviations of metabolites and acquired *m*/*z* values are included in Supporting Information 8.

pH 7.0) at 37 °C and 200 rpm (New Bruinswick Innova 44R, Eppendorf, Hamburg, Germany).

MLP were derived from 4 different sources as indicated in Table 1. Genes were codon optimized for *P. chrysogenum*, and ordered as synthetic DNA (IDT, Leuven, Belgium). Subcloning into the pIAT or pACYCtac vector was done using restriction with NdeI and NsiI. Assembled constructs were sequence-verified using Sanger sequencing (Macrogen, The Nether-

DOI: 10.1021/acssynbio.9b00106
ACS Synth. Biol. 2019, 8, 1776−1787

lands). The *N. lactamdurans* ACVS gene was kindly provided by DSM-Sinochem Pharmaceuticals B.V.

For targeted integration of ComB MLP, the MoClo combinatorial cloning system[55] was used to build a final level 2 construct (pCP-*com*-ergA) by combining the Com expression cassette from pACYCtac-*com* and the squalene epoxidase *ergA* (Pc22g15550, expressed by the widely used *pgpdA* promoter from *Aspergillus nidulans*) to confer resistance to terbinafine[56] as transcriptional units TU1 and TU2, respectively. The obtained plasmid pCP-*com*-ergA served as a template for donor DNA amplification with 100bp-IGR-MoClo-FW and 100bp-IGR-MoClo-R, adding 100 bp homology to facilitate integration onto the intergenic region between Pc20g07090 and Pc20g07100.

Transformation of MLP into *P. chrysogenum*. For initial transformations that introduced MLPs into *P. chrysogenum*, pIAT-MLP plasmids were cut with NotI and *Sma*I, recovered from gel, purified, and subsequently concentrated by desalting. Protoplasts were prepared as described.[57] Co-transformation was performed using the obtained MLP expression cassette together with linearized pDONR221AMDS marker vector in a ratio of 1:10. For targeted integrated of ComB MLP, donor DNA was PCR-amplified from pCP-*com*-ergA with primer IGR-FW and IGR-R, purified, and 4 μg were used for transformations. To enhance homologous recombination into the accessible intergenic region between Pc20g07090 and Pc20g07100,[58] 3 sgRNAs (Supporting Information 10) were used for formation of Cas9 ribonuclear protein particles as described previously.[45]

After 5−7 days, colonies were screened for integration of the MLP expression cassette with primers (Sigma-Aldrich, Zwijndrecht, The Netherlands) (Supporting Information 10) targeting the IPNS promoter and the AT terminator of each MLP expression cassette using colony PCR (Phire Plant Direct PCR Kit, Thermo Fisher Scientific, Bleiswijk, The Netherlands). Positive colonies were purified using three sporulation-selection transfer cycles before rice batches for storage and inoculation of shake-flasks were prepared.

Cultivation of *P. chrysogenum*. *Penicillium* strains carrying the MLP genes were subjected to shake-flask cultivation experiments for up to 5 days. For preculture, spores stored on rice grains were inoculated in 25 mL YGG medium. After 24 h, the sporulated preculture was 10-fold diluted in a total volume of 30 mL Penicillin production medium,[59] which was supplemented with phenylacetic acid (PAA) when the penicillin BGC was present in the strains to produce penicillin G. All cultures were grown at 25 °C and 200 rpm under semidark conditions in standard laboratory shakers (Innova44, New Brunswick Scientific, Nijmegen, The Netherlands). Sampling was performed on day 2 and day 5 after preculture transfer by aseptically harvesting 2 mL of culture from the shake flask followed by centrifugation at 4 °C and 14 000*g* for 10 min to pellet mycelium. From four strains expressing the MLP ComB, mycelium was mixed with Trizol reagent (Thermo Fisher Scientific, Bleiswijk, The Netherlands), transferred to screw-cap tubes containing glass beads (0.75−1 mm, Sigma-Aldrich, Zwijndrecht, The Netherlands) and stored at −80 °C until analysis. The supernatant was subsequently filtered using a 0.2 μM PTFE membrane syringe filter (VWR, Amsterdam, The Netherlands) and stored at −80 °C up until analysis. Samples were reduced using 10 mM TCEP prior to analysis. The remaining volume of the culture after 5 days was additionally used for dry weight determination. In all experiments two biological and two technical replicates were used.

qPCR Analysis of Gene Copy Number and NRPS Expression in MLP Strains. Mycelium stored in Trizol was disrupted with a FastPrep FP120 system (Qbiogene, Cedex, France). Total RNA was isolated from aqueous phase by chloroform/Isopropanol isolation and purified using the Ambion Turbo DNA free kit (Thermo Fisher Scientific, Bleiswijk, The Netherlands). RNA degradation was analyzed by electrophoresis using a 2% agarose gel and concentrations were determined with a NanoDrop ND 1000 (ISOGEN, Utrecht, The Netherlands). The iScript cDNA synthesis kit (Bio Rad, The Netherlands) was used for reverse transcription with 500 ng total RNA as input. The primers used for qPCR of Pc21g21390 (*pcbAB*), Pc21g15480 (*roqA*), Pc21g12630 (*chyA*), and ComB are listed in (Supporting Information 2). The γ actin gene (*Pc20g11630*) was used as internal standard for data normalization. SensiMix SYBR Hi ROX (Bioline Reagents, England) was used as master mix for qPCR. All runs were performed on a MiniOpticon system (Bio Rad) with two technical replicates per strain. The following conditions were employed for amplification: 95 °C for 10 min, followed by 40 cycles of 95 °C for 15 s, 60 °C for 30 s and 72 °C for 30 s, following an acquisition step. Raw ct data were exported and analysis of relative gene expression was performed with the $2-\Delta\Delta CT$ method.[60]

The copy number of *pcbAB* and the MLP homologue ComB was determined from isolated genomic DNA of a selection of strains, following the same protocols of qPCR as described above. For normalization and reference point of single copy, γ actin was used.

LC−MS Analysis and Evaluation of Metabolite Profiles. Clarified culture broth samples from fermentations were subjected to LC-HRMS analysis. Analysis was performed by injecting 5 μL sample on a C18 column (Shim-pack XR-ODS 2.2; 3.0 × 75 mm, Shimadzu, Japan) coupled to a Orbitrap Exactive (Thermo Fisher Scientific, The Netherlands) operated in positive ionization mode. A gradient program with water (A), acetonitrile (B), and 2% formic acid in water (C) was run; 0 min; A 90%, B 5%, C 5%; 4 min, A 90%, B 5%, C 5%; 13 min, A 0%, B 95%, C 5%; 16 min A 0%, B 95%, C 5%; 16 min, A 90%, B 5%, C 5%; 20 min A 90%, B 5%, C 5% at a flow rate of 0.3 mL min^{-1}. Two technical replicates were recorded for each sample. Available standards were used to identify peaks according to retention time and accurate mass. A complete list of all metabolites and intermediates which were identified is summarized in Supporting Information 8.

■ ASSOCIATED CONTENT

Supporting Information

The Supporting Information is available free of charge on the ACS Publications website at DOI: 10.1021/acssynbio.9b00106.

Proteins templates used as input for structure-based models; Quality parameter results of structural models built for fungal A-domains and MLPs; Quality parameter results of structural alignment of fungal A-domains and MLPs with SlgN1; MLPs copurify with full-length ACVS; Colony PCR results confirm integration of MLP expression cassettes in DS24742; Total Ion current (TIC) of DS47274 (A) and DS17690 (B) with and without the Com MLP; Expression changes in NRPS genes measured by qPCR; Measured metabolites of

DOI: 10.1021/acssynbio.9b00106
ACS Synth. Biol. 2019, 8, 1776−1787

biosynthetic pathways covered in this study; Overview of *P. chrysogenum* strains used in this study; List of primers and sgRNAs used in this study (PDF)

AUTHOR INFORMATION

Corresponding Author

*E-mail: a.j.m.driessen@rug.nl. Tel: (31) 50 363 2164.

ORCID

Arnold J. M. Driessen: 0000-0001-9258-9104

Present Address

[‖]Department of Applied and Molecular Microbiology, Institute of Biotechnology, Technische Universität Berlin, 10623 Berlin, Germany.

Author Contributions

R.D.Z. and A.J.M.D. designed the experiments. R.D.Z. and C.P. performed the experiments under supervision of A.J.M.D. and R.A.L.B.; R.D.Z. and C.P. wrote the manuscript with the improvements and directions from A.J.M.D and R.A.L.B. All authors read and approved the final manuscript.

Notes

The authors declare the following competing financial interest(s): A Patent (WO2017178624A1) has been published covering the application of MbtH-like proteins in eukaryotic NRPS-catalyzed processes.

ACKNOWLEDGMENTS

The research leading to these results was financially supported by the BE-Basic Foundation (Biotechnology based Ecologically Balanced Sustainable Industrial Consortium), and the European Commission's Marie Curie Initial Training Network Quantfung (FP7-People-2013-ITN, Grant No. 607332). The authors would like to thank Ulrike M. Müller for valuable suggestions and intellectual support in this study.

ABBREVIATIONS

BGC, biosynthetic gene cluster; NRPS, nonribosomal peptide synthase; ACVS, L-δ-(α-aminoadipyl)-L-cysteinyl-D-valine synthetase; LLD-ACV, L-δ-(α-aminoadipyl)-L-cysteinyl-D-valine; PK, polyketide; NRP, nonribosomal peptide; Pptases, 4′-phosphopantetheinyl-transferases; MLPs, MbtH-like proteins; A-domain, adenylation domain; GMQE, Global Model Quality Estimate; RMSD, Root Mean Square Deviation; 6-APA, 6-Aminopenicillanic acid; PDB, RCSB Protein Data Bank ID; CSI, classical strain improvement program

REFERENCES

(1) Marahiel, M. A., Stachelhaus, T., and Mootz, H. D. (1997) Modular Peptide Synthetases Involved in Nonribosomal Peptide Synthesis. *Chem. Rev. 2665* (96), 2651.

(2) Smith, J. L., and Sherman, D. H. (2008) An Enzyme Assembly Line. *Science (Washington, DC, U. S.) 321* (5894), 1304−1305.

(3) Weber, T., and Marahiel, M. A. (2001) Exploring the Domain Structure of Modular Nonribosomal Peptide Synthetases. *Structure 9* (1), R3−R9.

(4) Caboche, S., Pupin, M., Leclère, V., Fontaine, A., Jacques, P., and Kucherov, G. (2007) NORINE: A Database of Nonribosomal Peptides. *Nucleic Acids Res. 36*, D326−D331.

(5) Caboche, S., Leclère, V., Pupin, M., Kucherov, G., and Jacques, P. (2010) Diversity of Monomers in Nonribosomal Peptides: Towards the Prediction of Origin and Biological Activity. *J. Bacteriol. 192* (19), 5143−5150.

(6) Dang, T., and Süssmuth, R. D. (2017) Bioactive Peptide Natural Products as Lead Structures for Medicinal Use. *Acc. Chem. Res. 50* (7), 1566−1576.

(7) Watanabe, K., Oguri, H., and Oikawa, H. (2009) Enzymatic Synthesis of Molecular Skeletons of Complex Antitumor Antibiotics with Non-Ribosomal Peptide Synthetases. *Yuki Gosei Kagaku Kyokaishi 67* (11), 1152−1160.

(8) Frisvad, J. C., Smedsgaard, J., Larsen, T. O., and Samson, R. A. (2004) Mycotoxins, Drugs and Other Extrolites Produced by Species in Penicillium Subgenus Penicillium. *Stud. Mycol.*, 201−241.

(9) Nakano, M. M., Corbell, N., Besson, J., and Zuber, P. (1992) Isolation and Characterization of Sfp: A Gene That Functions in the Production of the Lipopeptide Biosurfactant, Surfactin, in Bacillus Subtilis. *Mol. Gen. Genet.*, 313−321.

(10) Beld, J., Sonnenschein, E. C., Vickery, C. R., Noel, J. P., and Burkart, M. D. (2014) The Phosphopantetheinyl Transferases: Catalysis of a Posttranslational Modification Crucial for Life. *Nat. Prod. Rep. 31* (1), 61−108.

(11) Chen, D., Wu, R., Bryan, T. L., and Dunaway-Mariano, D. (2009) In Vitro Kinetic Analysis of Substrate Specificity in Enterobactin Biosynthetic Lower Pathway Enzymes Provides Insight into the Biochemical Function of the Hot Dog-Fold Thioesterase EntH. *Biochemistry 48* (3), 511−513.

(12) Lauer, B., Russwurm, R., Schwarz, W., Kálmánczhelyi, A., Bruntner, C., Rosemeier, A., and Bormann, C. (2001) Molecular Characterization of Co-Transcribed Genes from Streptomyces Tendae Tü901 Involved in the Biosynthesis of the Peptidyl Moiety and Assembly of the Peptidyl Nucleoside Antibiotic Nikkomycin. *Mol. Gen. Genet. 264* (5), 662−673.

(13) Felnagle, E. A., Barkei, J. J., Park, H., Podevels, A. M., McMahon, M. D., Drott, D. W., and Thomas, M. G. (2010) MbtH-like Proteins as Integral Components of Bacterial Nonribosomal Peptide Synthetases. *Biochemistry 49* (41), 8815−8817.

(14) Boll, B., Taubitz, T., and Heide, L. (2011) Role of MbtH-like Proteins in the Adenylation of Tyrosine during Aminocoumarin and Vancomycin Biosynthesis. *J. Biol. Chem. 286* (42), 36281−36290.

(15) Zhang, W., Heemstra, J. R., Walsh, C. T., and Imker, H. J. (2010) Activation of the Pacidamycin PacI Adenylation Domain by MbtH-like Proteins. *Biochemistry 49* (46), 9946−9947.

(16) Rusnak, F., Sakaitani, M., Drueckhammer, D., Reichert, J., and Walsh, C. T. (1991) Biosynthesis of the Escherichia Coli Siderophore Enterobactin: Sequence of the EntF Gene, Expression and Purification of EntF, and Analysis of Covalent Phosphopantetheine. *Biochemistry 30* (11), 2916−2927.

(17) Quadri, L. E. N., Sello, J., Keating, T. A., Weinreb, P. H., and Walsh, C. T. (1998) Identification of a Mycobacterium Tuberculosis Gene Cluster Encoding the Biosynthetic Enzymes for Assembly of the Virulence-Conferring Siderophore Mycobactin. *Chem. Biol. 5* (11), 631−645.

(18) Ochsner, U. A., Wilderman, P. J., Vasil, A. I., and Vasil, M. L. (2002) Gene Chip Expression Analysis of the Iron Starvation Response in Pseudomonas Aeruginosa: Identification of Novel Pyoverdine Biosynthesis Genes. *Mol. Microbiol. 45* (5), 1277−1287.

(19) Lautru, S., Oves-Costales, D., Pernodet, J. L., and Challis, G. L. (2007) MbtH-like Protein-Mediated Cross-Talk between Non-Ribosomal Peptide Antibiotic and Siderophore Biosynthetic Pathways in Streptomyces Coelicolor M145. *Microbiology 153* (5), 1405−1412.

(20) Wolpert, M., Gust, B., Kammerer, B., and Heide, L. (2007) Effects of Deletions of MbtH-like Genes on Clorobiocin Biosythesis in Streptomyces Coelicolor. *Microbiology 153* (5), 1413−1423.

(21) Esquilín-Lebrón, K. J., Boynton, T. O., Shimkets, L. J., and Thomas, M. G. (2018) An Orphan MbtH-Like Protein Interacts with Multiple Nonribosomal Peptide Synthetases in Myxococcus Xanthus DK1622. *J. Bacteriol. 200* (21), 1−13.

(22) Felnagle, E. A., Barkei, J. J., Park, H., Podevels, A. M., McMahon, M. D., Drott, D. W., and Thomas, M. G. (2010) MbtH-like Proteins as Integral Components of Bacterial Nonribosomal Peptide Synthetases. *Biochemistry 49* (41), 8815−8817.

DOI: 10.1021/acssynbio.9b00106
ACS Synth. Biol. 2019, 8, 1776−1787

(23) Stegmann, E., Rausch, C., Stockert, S., Burkert, D., and Wohlleben, W. (2006) The Small MbtH-like Protein Encoded by an Internal Gene of the Balhimycin Biosynthetic Gene Cluster Is Not Required for Glycopeptide Production. *FEMS Microbiol. Lett. 262*, 85−92.
(24) van den Berg, M. A., Albang, R., Albermann, K., Badger, J. H., Daran, J.-M., Driessen, A. J. M., Garcia-Estrada, C., Fedorova, N. D., Harris, D. M., Heijne, W. H. M., et al. (2008) Genome Sequencing and Analysis of the Filamentous Fungus Penicillium Chrysogenum. *Nat. Biotechnol. 26* (10), 1161−1168.
(25) van den Berg, M. A. (2011) Impact of the Penicillium Chrysogenum Genome on Industrial Production of Metabolites. *Appl. Microbiol. Biotechnol. 92* (1), 45−53.
(26) Herbst, D. A., Boll, B., Zocher, G., Stehle, T., and Heide, L. (2013) Structural Basis of the Interaction of Mbth-like Proteins, Putative Regulators of Nonribosomal Peptide Biosynthesis, with Adenylating Enzymes. *J. Biol. Chem. 288* (3), 1991−2003.
(27) Miller, B. R., Drake, E. J., Shi, C., Aldrich, C. C., and Gulick, A. M. (2016) Structures of a Nonribosomal Peptide Synthetase Module Bound to MbtH-like Proteins Support a Highly Dynamic Domain Architecture. *J. Biol. Chem. 291* (43), 22559−22571.
(28) Drake, E. J., Miller, B. R., Shi, C., Tarrasch, J. T., Sundlov, J. A., Leigh Allen, C., Skiniotis, G., Aldrich, C. C., and Gulick, A. M. (2016) Structures of Two Distinct Conformations of Holo-Non-Ribosomal Peptide Synthetases. *Nature 529* (7585), 235−238.
(29) Mori, S., Pang, A. H., Lundy, T. A., Garzan, A., Tsodikov, O. V., and Garneau-Tsodikova, S. (2018) Structural Basis for Backbone N-Methylation by an Interrupted Adenylation Domain. *Nat. Chem. Biol. 14* (5), 428−430.
(30) Tarry, M. J., Haque, A. S., Bui, K. H., and Schmeing, T. M. (2017) X-Ray Crystallography and Electron Microscopy of Cross- and Multi-Module Nonribosomal Peptide Synthetase Proteins Reveal a Flexible Architecture. *Structure 25* (5), 783−793.
(31) Tahlan, K., Moore, M. A., and Jensen, S. E. (2017) δ-(l-α-Aminoadipyl)-l-Cysteinyl-d-Valine Synthetase (ACVS): Discovery and Perspectives. *J. Ind. Microbiol. Biotechnol. 44* (4−5), 517−524.
(32) Byford, M. F., Baldwin, J. E., Shiau, C.-Y., and Schofield, C. J. (1997) The Mechanism of ACV Synthetase. *Chem. Rev. 97* (7), 2631−2650.
(33) van Liempt, H., von Dohren, H., and Kleinkauf, H. (1989) Delta-(L-Alpha-Aminoadipyl)-L-Cysteinyl-D-Valine Synthetase from Aspergillus Nidulans. The First Enzyme in Penicillin Biosynthesis Is a Multifunctional Peptide Synthetase. *J. Biol. Chem. 264* (7), 3680−3684.
(34) Ries, M. I., Ali, H., Lankhorst, P. P., Hankemeier, T., Bovenberg, R. A. L., Driessen, A. J. M., and Vreeken, R. J. (2013) Novel Key Metabolites Reveal Further Branching of the Roquefortine/ Meleagrin Biosynthetic Pathway. *J. Biol. Chem. 288* (52), 37289−37295.
(35) Ali, H., Ries, M. I., Nijland, J. G., Lankhorst, P. P., Hankemeier, T., Bovenberg, R. A. L., Vreeken, R. J., and Driessen, A. J. M. (2013) A Branched Biosynthetic Pathway Is Involved in Production of Roquefortine and Related Compounds in Penicillium Chrysogenum. *PLoS One 8* (6), No. e65328.
(36) Zheng, C. J., Sohn, M., Lee, S., and Kim, W. (2013) Meleagrin, a New FabI Inhibitor from Penicillium Chryosogenum with at Least One Additional Mode of Action. *PLoS One 8* (11), e78922.
(37) Garcia-Estrada, C., Ullan, R. V., Albillos, S. M., Fernandez-Bodega, M. A., Durek, P., von Dohren, H., and Martin, J. F. (2011) A Single Cluster of Coregulated Genes Encodes the Biosynthesis of the Mycotoxins Roquefortine C and Meleagrin in Penicillium Chrysogenum. *Chem. Biol. 18* (11), 1499−1512.
(38) Ames, B. D., and Walsh, C. T. (2010) Anthranilate-Activating Modules from Fungal Nonribosomal Peptide Assembly Lines. *Biochemistry 49*, 3351−3365.
(39) Viggiano, A., Salo, O., Ali, H., Szymanski, W., Lankhorst, P. P., Nygård, Y., Bovenberg, R. A. L., and Driessen, A. J. M. (2018) Pathway for the Biosynthesis of the Pigment Chrysogine by Penicillium Chrysogenum. *Appl. Environ. Microbiol. 84* (4), 1−11.
(40) Wollenberg, R. D., Saei, W., Westphal, K. R., Klitgaard, C. S., Nielsen, K. L., Lysøe, E., Gardiner, D. M., Wimmer, R., Sondergaard, T. E., and Sørensen, J. L. (2017) Chrysogine Biosynthesis Is Mediated by a Two-Module Nonribosomal Peptide Synthetase. *J. Nat. Prod. 80*, 2131−2135.
(41) Schomer, R. A., and Thomas, M. G. (2017) Characterization of the Functional Variance in MbtH-like Protein Interactions with a Nonribosomal Peptide Synthetase. *Biochemistry 56* (40), 5380−5390.
(42) Salo, O., Guzmán-Chávez, F., Ries, M. I., Lankhorst, P. P., Bovenberg, R. A. L., Vreeken, R. J., and Driessen, A. J. M. (2016) Identification of a Polyketide Synthase Involved in Sorbicillin Biosynthesis by Penicillium Chrysogenum. *Appl. Environ. Microbiol. 82* (13), 3971−3978.
(43) Guzmán-Chávez, F., Salo, O., Nygård, Y., Lankhorst, P. P., Bovenberg, R. A. L., and Driessen, A. J. M. (2017) Mechanism and Regulation of Sorbicillin Biosynthesis by Penicillium Chrysogenum. *Microb. Biotechnol. 10* (4), 958−968.
(44) Ali, H., Ries, M. I., Lankhorst, P. P., Van Der Hoeven, R. A. M., Schouten, O. L., Noga, M., Hankemeier, T., Van Peij, N. N. M. E., Bovenberg, R. A. L., and Vreeken, R. J. (2014) A Non-Canonical NRPS Is Involved in the Synthesis of Fungisporin and Related Hydrophobic Cyclic Tetrapeptides in Penicillium Chrysogenum. *PLoS One 9* (6), e98212.
(45) Pohl, C., Kiel, J. A. K. W., Driessen, A. J. M., Bovenberg, R. A. L., and Nygård, Y. (2016) CRISPR/Cas9 Based Genome Editing of Penicillium Chrysogenum. *ACS Synth. Biol. 5* (7), 754−764.
(46) Polli, F., Meijrink, B., Bovenberg, R. A. L., and Driessen, A. J. M. (2016) New Promoters for Strain Engineering of Penicillium Chrysogenum. *Fungal Genet. Biol. 89*, 62−71.
(47) Harris, D. M., van der Krogt, Z. A., Klaassen, P., Raamsdonk, L. M., Hage, S., van den Berg, M. A., Bovenberg, R. A. L., Pronk, J. T., and Daran, J. M. (2009) Exploring and Dissecting Genome-Wide Gene Expression Responses of Penicillium Chrysogenum to Phenylacetic Acid Consumption and PenicillinG Production. *BMC Genomics 10*, 1−20.
(48) Esquilín-Lebrón, K. J., Boynton, T. O., Shimkets, L. J., and Thomas, M. G. (2018) An Orphan MbtH-Like Protein Interacts with Multiple Nonribosomal Peptide Synthetases in Myxococcus Xanthus DK1622. *J. Bacteriol.*, DOI: 10.1128/JB.00346-18.
(49) Marchler-Bauer, A., Derbyshire, M. K., Gonzales, N. R., Lu, S., Chitsaz, F., Geer, L. Y., Geer, R. C., He, J., Gwadz, M., Hurwitz, D. I., et al. (2015) CDD: NCBI's Conserved Domain Database. *Nucleic Acids Res. 43* (D1), D222−D226.
(50) Källberg, M., Wang, H., Wang, S., Peng, J., Wang, Z., Lu, H., and Xu, J. (2012) Template-Based Protein Structure Modeling Using the RaptorX Web Server. *Nat. Protoc. 7* (8), 1511−1522.
(51) Biasini, M., Bienert, S., Waterhouse, A., Arnold, K., Studer, G., Schmidt, T., Kiefer, F., Cassarino, T. G., Bertoni, M., Bordoli, L., et al. (2014) SWISS-MODEL: Modelling Protein Tertiary and Quaternary Structure Using Evolutionary Information. *Nucleic Acids Res. 42* (W1), 1−7.
(52) Schrödinger, LLC. (2015) *The {PyMOL} Molecular Graphics System*, Version 1.8.
(53) Segura, J., Sanchez-Garcia, R., Tabas-Madrid, D., Cuenca-Alba, J., Sorzano, C. O. S., and Carazo, J. M. (2016) 3DIANA: 3D Domain Interaction Analysis: A Toolbox for Quaternary Structure Modeling. *Biophys. J. 110* (4), 766−775.
(54) Gruenewald, S., Mootz, H. D., Stehmeier, P., and Stachelhaus, T. (2004) In Vivo Production of Artificial Nonribosomal Peptide Products in the Heterologous Host Escherichia Coli. *Appl. Envrion. Microbiol. 70* (6), 3282−3291.
(55) Weber, E., Engler, C., Gruetzner, R., Werner, S., and Marillonnet, S. (2011) A Modular Cloning System for Standardized Assembly of Multigene Constructs. *PLoS One 6* (2), e16765.
(56) Sigl, C., Handler, M., Sprenger, G., Kürnsteiner, H., and Zadra, I. (2010) A Novel Homologous Dominant Selection Marker for Genetic Transformation of Penicillium Chrysogenum: Overexpression of Squalene Epoxidase-Encoding ErgA. *J. Biotechnol. 150* (3), 307−311.

DOI: 10.1021/acssynbio.9b00106
ACS Synth. Biol. 2019, 8, 1776−1787

(57) Kovalchuk, A., Weber, S. S., Nijland, J. G., Bovenberg, R. A. L., and Driessen, A. J. M. (2012) Fungal ABC Transporter Deletion and Localization Analysis. *Methods Mol. Biol. 835*, 1−16.
(58) Polli, F., Meijrink, B., Bovenberg, R. A. L., and Driessen, A. J. M. (2016) New Promoters for Strain Engineering of Penicillium Chrysogenum. *Fungal Genet. Biol. 89*, 62−71.
(59) Kovalchuk, A., Weber, S. S., Nijland, J. G., Bovenberg, R. A. L., and Driessen, A. J. M. (2012) Fungal ABC Transporter Deletion and Localization Analysis. *Methods Mol. Biol. 835*, 1−16.
(60) Livak, K. J., and Schmittgen, T. D. (2001) Analysis of Relative Gene Expression Data Using Real-Time Quantitative PCR and the 2-ΔΔCT Method. *Methods 25* (4), 402−408.
(61) Chiu, H. T., Hubbard, B. K., Shah, A. N., Eide, J., Fredenburg, R. A., Walsh, C. T., and Khosla, C. (2001) Molecular Cloning and Sequence Analysis of the Complestatin Biosynthetic Gene Cluster. *Proc. Natl. Acad. Sci. U. S. A. 98* (15), 8548−8553.
(62) Bentley, S., Chater, K., Cerdeño-Tárraga, A.-M., Challis, G. L., Thomson, N. R., James, K. D., Harris, D. E., Quail, M. A., Kieser, H., Harper, D., et al. (2002) Complete Genome Sequence of the Model Actinomycete Streptomyces Coelicolor A3(2). *Nature 417* (6885), 141−147.
(63) Sosio, M., Kloosterman, H., Bianchi, A., de Vreugd, P., Dijkhuizen, L., and Donadio, S. (2004) Organization of the Teicoplanin Gene Cluster in Actinoplanes Teichomyceticus. *Microbiology 150* (1), 95−102.
(64) Banik, J. J., and Brady, S. F. (2008) Cloning and Characterization of New Glycopeptide Gene Clusters Found in an Environmental DNA Megalibrary. *Proc. Natl. Acad. Sci. U. S. A. 105* (45), 17273−17277.
(65) Baltz, R. H. (2011) Function of MbtH Homologs in Nonribosomal Peptide Biosynthesis and Applications in Secondary Metabolite Discovery. *J. Ind. Microbiol. Biotechnol. 38* (11), 1747−1760.
(66) Szklarczyk, D., Franceschini, A., Wyder, S., Forslund, K., Heller, D., Huerta-Cepas, J., Simonovic, M., Roth, A., Santos, A., Tsafou, K. P., et al. (2015) STRING V10: Protein-Protein Interaction Networks, Integrated over the Tree of Life. *Nucleic Acids Res. 43* (D1), D447−D452.

DOI: 10.1021/acssynbio.9b00106
ACS Synth. Biol. 2019, 8, 1776−1787